ZnO 1-D nanostructures: Low temperature synthesis and characterizations

APURBA DEV, S CHAUDHURI[†] and B N DEV*

Department of Materials Science, Indian Association for the Cultivation of Science, Jadavpur, Kolkata 700 032, India

Abstract. ZnO is one of the most important semiconductors having a wide variety of applications in photonic, field emission and sensing devices. In addition, it exhibits a wide variety of morphologies in the nano regime that can be grown by tuning the growth habit of the ZnO crystal. Among various nanostructures, oriented 1-D nanoforms are particularly important for applications such as UV laser, sensors, UV LED, field emission displays, piezoelectric nanogenerator etc. We have developed a soft chemical approach to fabricate well-aligned arrays of various 1-D nanoforms like nanonails, nanowires and nanorods. The microstructural and photoluminescence properties of all the structures were investigated and tuned by varying the synthesis parameters. Field emission study from the aligned nanorod arrays exhibited high current density and a low turn-on field. These arrays also exhibited very strong UV emission and week defect emission. These structures can be utilized to fabricate efficient UV LEDs.

Keywords. Aligned 1-D ZnO nanostructures; surfactant mediated growth; optical absorption and emission; field emission properties.

1. Introduction

Zinc oxide is an outstanding semiconductor having a wide bandgap energy of 3·37 eV and a large excitonic binding energy (60 meV) at room temperature. The excitonic binding energy of ZnO is much higher than the thermal energy at room temperature (26 meV), and it is also much higher than those of other prospective materials such as ZnSe (22 meV), ZnS (40 meV), and GaN (25 meV), which make it one of the outstanding semiconductors for lasing. The lack of centre of symmetry in wurtzite crystals and large electrochemical coupling result in strong piezoelectric and pyroelectric properties in ZnO which have important applications like mechanical actuators and piezoelectric sensors (Wang 2004). In addition, ZnO exhibits a diverse group of growth morphologies in the nano regime that has made this material a promising candidate in the field of nanotechnology. Among the various nanoforms, one-dimensional oriented nanostructures such as nanorods, nanowires, nanotubes, nanopins etc are particularly important for efficient field emission that has enormous commercial applications like field emission flat panel displays (Baughman *et al* 2002), X-ray sources (Senda *et al* 2004), vacuum microwave amplifiers (Saito and Uemura 2000; Milne *et al* 2004) etc. With their high melting point, good thermal and chemical stability and low electron affinity (Fancher *et al* 1998), ZnO one-dimensional

arrays are promising alternatives to carbon nanotubes (CNT) for field emitters with long lifetimes. Moreover, the successful demonstration of UV lasing action (Huang *et al* 2001) from ZnO has added a new direction in the field of nanotechnology and motivated subsequent research for the fabrication of one-dimensional ZnO nanostructured arrays with precise control over size, shape and orientations. The ability to build oriented assemblies of 1-D nanostructures is also very attractive for the fabrication of future photonic (Wang *et al* 2004; Pan *et al* 2005), field emission (Li *et al* 2004) and sensing (Kar *et al* 2006) devices. As a consequence, several synthetic methodologies have been proposed. Gas phase growth techniques like chemical vapour deposition (CVD), physical vapour deposition (PVD), metalorganic vapour phase epitaxy (MOVPE) and vapour liquid–solid (VLS) etc (Park *et al* 2002; Lyu *et al* 2003; Bae *et al* 2004; Gao and Wang 2004) have been successfully employed to grow ZnO nanorods and nanowires on solid substrates. However, these methods are very expensive and require high temperature. Recently, solution phase approach to fabricate aligned ZnO nanorods was utilized (Guo *et al* 2002; Greene *et al* 2003; Li *et al* 2004; Li Q *et al* 2005; Yu *et al* 2005; Dev *et al* 2006). This technique has many advantages as it is cost-effective and large scale-up production is possible. In addition, oriented seed-initiated synthesis (Greene *et al* 2005) has been found to be very effective to produce highly aligned ZnO nanorod arrays. This technique (Greene *et al* 2005) is suitable for preparing long free-standing ZnO nanorods which exhibit efficient field emission, as long as their aspect ratio is high. But the increase in length is generally accompanied by subsequent increase in diameter. So, if a

---

*Author for correspondence
(msbnd@iacs.res.in; dev_apurba@yahoo.com)
[†]Since deceased

proper approach is adopted to restrict the lateral growth without affecting the orientation of the nanorods they could be expected to exhibit efficient field emission properties for their high aspect ratio and excellent orientation. In addition, the ability to choose crystallographic growth direction of a nanorod array aid in tuning the physical properties of the material, including spontaneous piezoelectric polarization, thermal and electrical conductivity, dielectric constant, lattice strain etc.

In this paper, we report a soft chemical approach to fabricate long and vertically aligned ZnO nanorod, nanowire and nanonail arrays with a specific crystallographic orientation, on sol–gel derived ZnO thin films. The role of different experimental parameters was explored with a view to achieve diameter controlled well-aligned ZnO nanorod arrays.

2. Experimental

2.1 *Preparation of ZnO film*

For the preparation of ZnO thin films, zinc acetate dihydrate [$Zn(CH_3COO)_2 \cdot 2H_2O$] was added in dry ethanol and subsequently a few drops of diethanolamine (DEA) were added with continuous stirring for 1 h. An optimized amount of basic DEA was added to the solution to enhance dissolution of the Zn-salt. Properly cleaned quartz, silicon and glass plates were used as the substrates. The substrates were coated with the sol by a dip coating technique and subsequently dried in an oven at 80°C for 5 min. This process was repeated 6 times to increase the film thickness and final films were annealed in air at 600°C for 30 min. The entire process was repeated three times again to ensure complete and uniform coverage of ZnO seeds. Finally, transparent ZnO films were obtained, which were utilized as the substrates for the formation of ZnO nanorod arrays.

2.2 *Preparation of ZnO nanorods*

For the preparation of ZnO nanorods, 10 mmol of sodium dodecyl sulphate (SDS) and 1 mmol of zinc acetate dihydrate were added to 30 ml of xylene and stirred for 1 h. Then hydrazine hydrate (80%) diluted with ethanol was added to the solution very slowly. After 1 h of stirring, previously prepared transparent ZnO films were immersed in the solution and refluxed at 90°C for 5 h. Finally, the substrates covered with a white layer were washed in distilled water and dried at room temperature. The films thus obtained were used for further characterization.

2.3 *Characterization*

The crystalline phase of the products was determined by X-ray powder diffraction by a Seifert 3000P diffractometer with CuKα radiation (λ = 1·54 Å). The compositional analysis was done by energy dispersive analysis of X-rays (EDAX, Kevex, Delta Class I). The morphology of the samples was determined by a scanning electron microscope (Hitachi; S-2300). Microstructure and crystal structures of the products were further studied with a high-resolution transmission electron microscope (HRTEM; JEOL 2010). Optical absorbance was recorded by a spectrophotometer (Hitachi, U-3410). Optical absorbance spectra of ZnO samples (both thin films and nanorod films) were directly measured by placing the films perpendicular to the direction of the incident light. Photoluminescence measurements were carried out with a luminescence spectrometer (Hitachi, FL 2500).
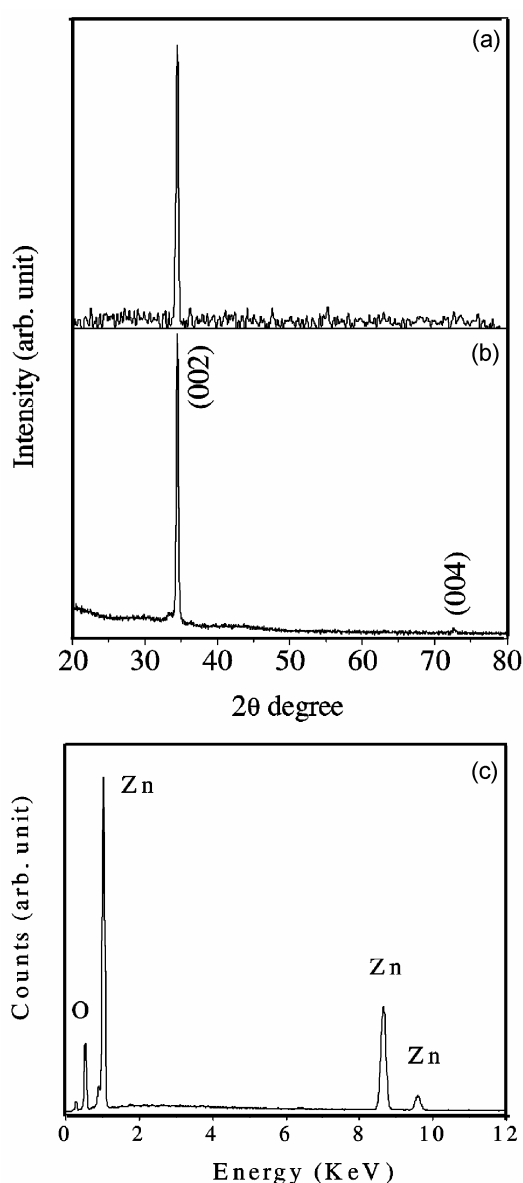

Figure 1. XRD pattern of (a) ZnO film on quartz substrate, (b) ZnO nanorod arrays and (c) EDAX pattern recorded over a representative ZnO nanorod array.

4. Results and discussion

X-ray diffraction (XRD) was performed on ZnO films both before and after the formation of nanorods. The XRD pattern of the transparent ZnO thin film prior to the nanorod growth is shown in figure 1a. A strong and sharp diffraction peak corresponding to the (002) crystal planes of ZnO, and absence of any other peak, revealed preferred orientation of the film with the *c*-axis of ZnO crystals aligned along the surface-normal to the substrate. It was observed that the results were independent of the substrates (silicon, quartz and glass) used. The XRD pattern (figure 1b) of the nanorod arrays indicates that the nanorods are well aligned and they grow along the [001] direction following the crystal orientation of the seed. The composition of the nanorods was determined by EDAX study (figure 1c) that revealed the presence of Zn and O as the elementary components in stoichiometric amount.

4.1 *Microstructural analysis*

Morphologies and dimensions of the nanorods were studied through SEM and TEM observations. Figure 2(a) shows SEM image of ZnO thin film revealing uniform distribution of ZnO seeds on a quartz substrate. Figure 2(b) is the low magnification image of the ZnO nanorod arrays showing uniformity of the nanorods over a large area. The image in the inset of figure 2(b) reveals the cross-section of the nanorods to be hexagonal. The image demonstrates that the orientation of the nanorods is quite good and the nanorods grow normal to the substrate. The nanorods have diameters ranging from 80–100 nm with lengths of ~ 3 μm. The magnified tilted view of the nanorods (figure 2c) reveals that the nanorods are well separated from each other.

With a view to investigate the role of the surfactant (SDS) and the base hydrazine hydrate over the dimension and degree of orientation of the ZnO nanorod arrays, we have carried out a series of experiments and the results are listed in table 1. ZnO nanorod arrays were also synthesized without using SDS following identical experimental procedure. It was observed that in all the cases the growth of the nanorods in the lateral dimensions were quite high. The SEM image shown in figure 3(a) reveals that the diameters of the resulting nanorods increased to around 500 nm within 2 h of refluxing. Thus these results indicated that the presence of the surfactant (SDS) was essential to regulate the lateral growth of ZnO nanorods.

Hydrazine hydrate is a strong base and it was used to regulate pH of the solution. The pH level of the reaction medium was also varied within a certain range keeping the amount of the surfactant and all other experimental parameters unchanged to investigate its effect on the ZnO nanorod arrays. Initially, pH of the solution was measured

to be 6·5 when hydrazine hydrate was not added. Experiment was also carried out at this condition keeping other parameters identical and the SEM studies of the resultant film revealed that ZnO nanorods did not grow on the ZnO coated substrate. In the next experiment, pH of the solution was raised to 10·6 by adding proper amount of hydrazine hydrate in the solution, which was then stirred for 1 h followed by 5 h refluxing. At this condition uniform growth of aligned and flexible ZnO nanowires having diameters, ~ 60 nm and lengths, ~ 2 μm, were observed (figure 3b). With further increase of the pH of the solu-
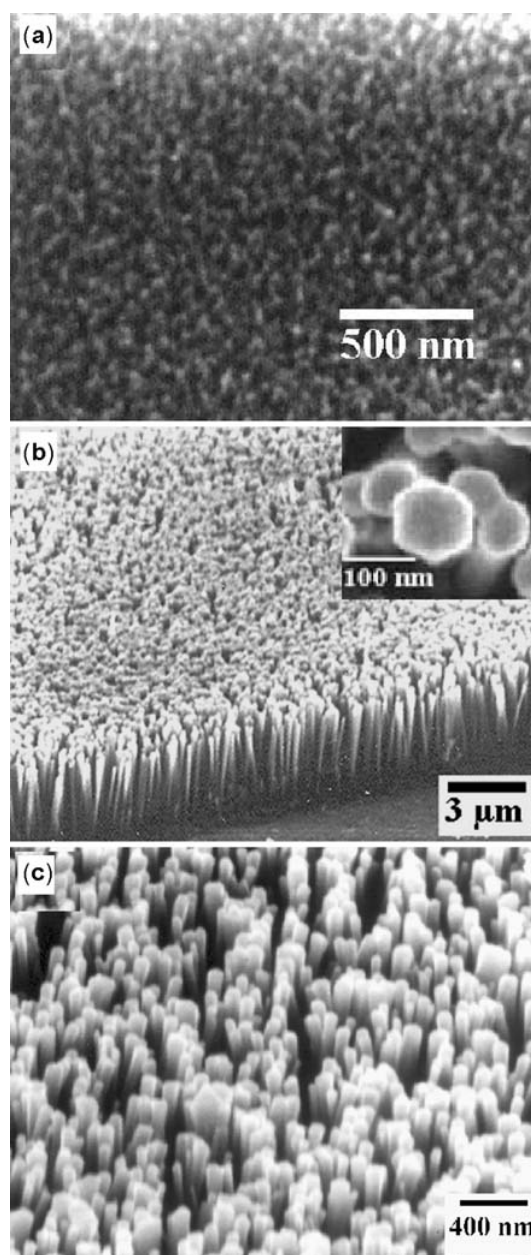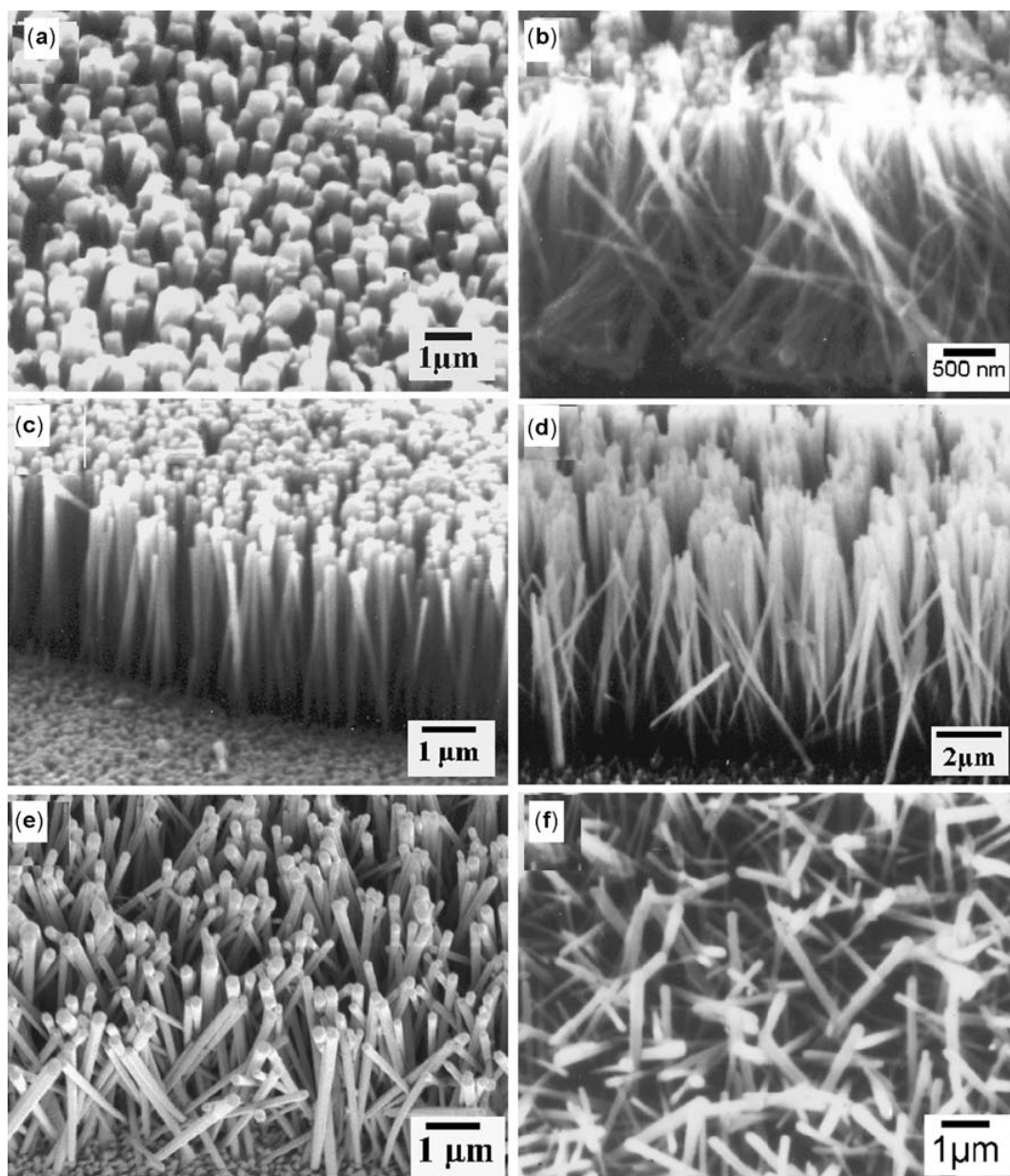

Figure 2. SEM image of (**a**) ZnO seed, (**b**) ZnO nanorod arrays over a large surface (inset shows the hexagonal tip of the nanorods) and (c) tilted view of the nanorod arrays.

Table 1.   Dependence of nanorod dimensions on pH, surfactant and reaction time.

Sample	pH of the solution	Surfactant	Reaction time (h)	Diameter of the nanorod (nm)	Length of the nanorod (μm)
S1	10·6	With SDS	5	~60	2
S2	11·3	With SDS	5	80–100	3
S3	11·6	With SDS	5	~120	6
S4	11·9	With SDS	3	200–250	3
S5	11·9	With SDS	5	200–250	7
S6	11·6	Without SDS	2	~500	2

Figure 3.   SEM images of nanorods prepared under different experimental conditions as listed in table 1: (**a**) S6, (**b**) S1, (**c**) S2, (**d**) S3, (**e**) S4 and (**f**) S5.

tion to 11·3, the resulting nanoforms were no more wire-like, instead they were rod-like having diameters around 80–100 nm while lengths increased to 3 μm (figure 3c).

There was a further increase in length and diameter when the pH of the solution was increased to 11·6. The SEM image of the sample prepared at this condition is shown

in figure 3d revealing the diameters of the nanorods to be ~ 120 nm and lengths, ~ 6 μm. It can be observed that the increase in lengths of the nanorods was much higher compared to their diameters with increasing pH level of the solution. Due to this abrupt increase in the length of the nanorods the freestanding nature of the nanorods were lost and instead they coalesced to each other at their tips. The diameter of the nanorods increased further to around 200–250 nm (figure 3e) within 3 h of refluxing when pH of the solution was raised to 11·9, but at this condition orientation of the nanorods collapsed resulting in the nonaligned products (figure 3e). A total collapse of the freestanding nature of the nanorods were noticed when the solution was refluxed for 5 h at this pH level (figure 3f). Close observation also revealed that the diameter of the nanorods prepared at pH level 11·6 or higher do not have uniform diameter along their length. The diameter is higher at the top and it is very thin at the bottom resulting in inverted nail like shape.

To investigate the effect of crystallographic orientation of ZnO thin films on the nanorods arrays, two experiments were carried out using ZnO thin films having no *c*-axis texturing effect. The pH of the solution was maintained at 11·3 and 11·6, respectively. The XRD pattern of ZnO thin film substrate and the as-prepared ZnO nanorod arrays are shown in figures 4a and b, respectively. It can be observed that in addition to the diffraction from (002) crystal planes a few more diffraction peaks of ZnO appeared in the XRD pattern of the ZnO thin film. However, in the nanorod samples these peaks were quite weak relative to the (002) peak. This could be attributed to the anisotropic growth of ZnO nanorods along [002] direction. The SEM images corresponding to pH 11·3 and 11·6 are shown in figures 5a and b, respectively. It can be observed that despite possessing quite identical diameters, the orientations of the nanorods prepared on the non *c*-axis oriented ZnO thin films (figures 5a and b) were poor compared to the samples, S2 and S3 (figures 3c and d, respectively) prepared with the *c*-axis oriented films under identical experimental conditions.

Transmission electron microscopy (TEM) was also performed to further investigate the size and crystallinity of the ZnO nanorods. Figure 6a shows the low magnification bright field TEM image of a single nanorod having a length of ~ 3 μm. The selected area electron diffraction (SAED) pattern (inset of figure 6a) reveals that the nanorod is single crystalline in nature. The lattice spacing estimated from the high resolution TEM image (figure 6b) of a single nanorod was found to be around 0·26 nm, which
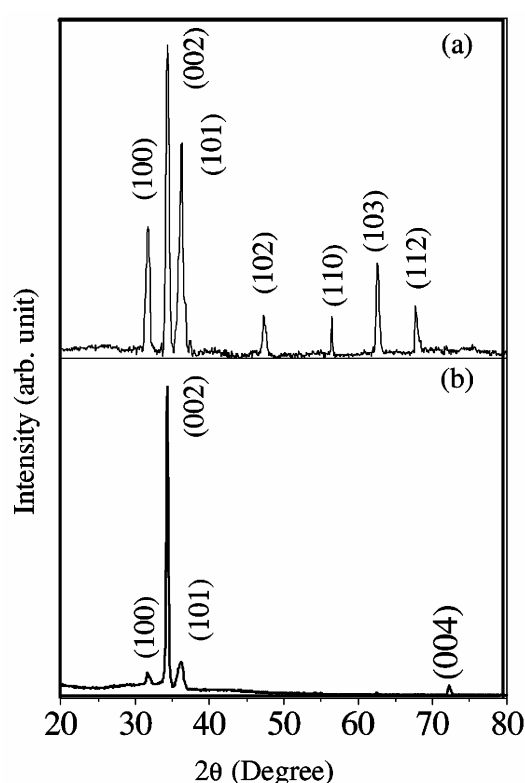

Figure 4. (a) XRD spectra of ZnO film having no preferred crystallographic orientation and (b) ZnO nanorod arrays prepared on the above ZnO film showing enhanced (001) orientation.
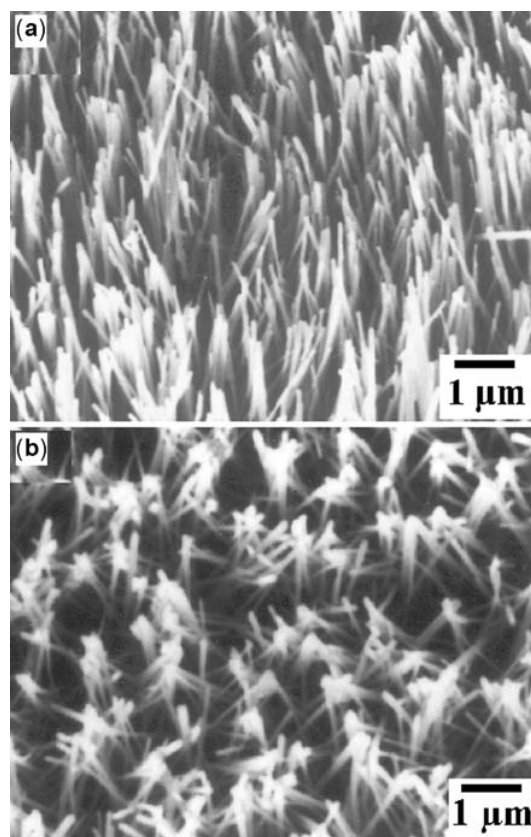

Figure 5. SEM image of the ZnO nanorod arrays prepared on ZnO film having no crystallographic orientation at pH value: (**a**) 11·3 and (**b**) 11·6.
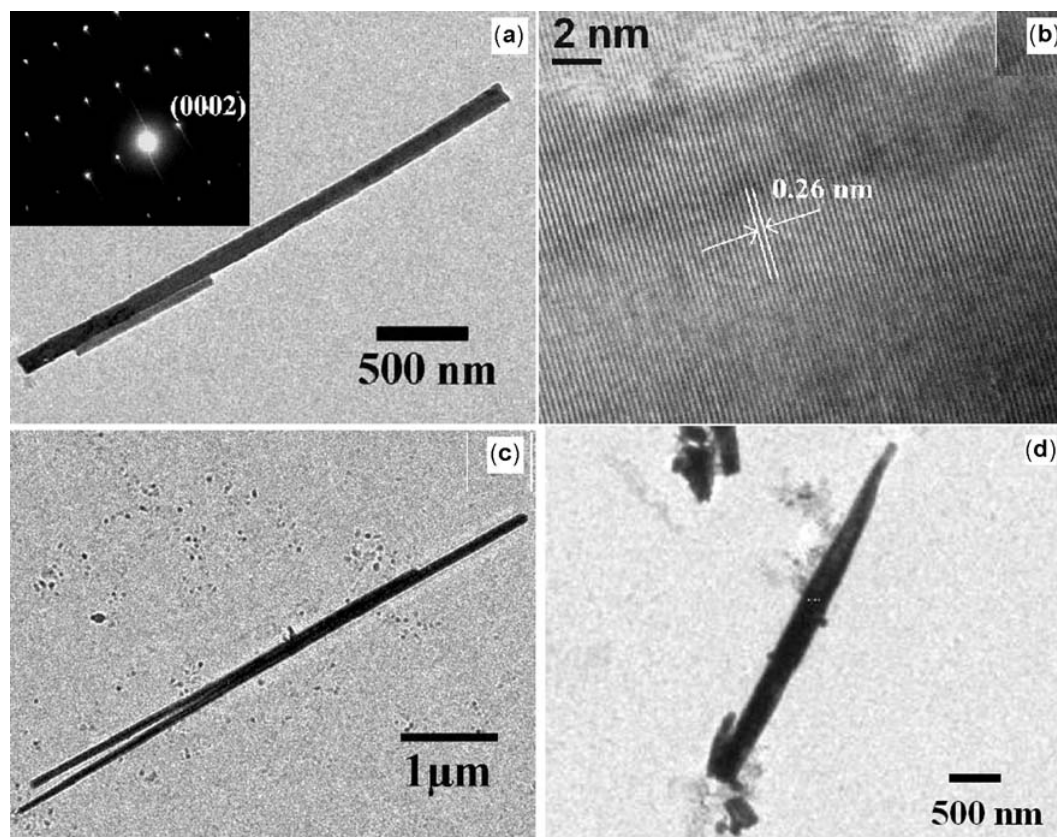
Figure 6. (**a**) TEM image of a single nanorod with the inset showing corresponding SAED pattern, (**b**) HRTEM image of a nanorod, (**c**) TEM image of a long nanorod (S3) and (**d**) TEM image of a nail like nanoform.

corresponds to the (002) planar spacing of ZnO in wurtzite phase. Figure 6c is the TEM image of nanorods formed in higher concentration of hydrazine hydrate (S3). It can be observed that the nanorods have lengths of ~ 6 μm and diameters of ~ 120 nm. Figure 6d shows the TEM image of a nail like nanoform.

4.2 *Growth mechanism*

In growing one-dimensional nanostructures, there are two important steps which control the quality of the products. The first one is the nucleation, which initiates the growth of 1-D nanostructures. In this synthesis process, *c*-axis oriented ZnO thin films were used. These seeded films served as nucleation sites and also provided a preferential crystallographic growth direction to the resulting nanorods. The second step is the growth, and for one-dimensional structure it is important to achieve anisotropic growth with good control over size, shape and orientation. The structure of ZnO wurtzite crystal can be described as a number of alternating planes composed of tetrahedrally coordinated O^{-2} and Zn^{2+} ions, stacked along *c*-axis (Wang 2004). These oppositely charged ions produce positively charged Zn-(001) and negatively charged O-(00-1) sur-

faces, resulting in a spontaneous polarization along *c*-axis. Due to this reason, ZnO surface attracts opposite charges (Zn^{2+} or OH^-) from the solution forming $Zn(OH)_2$. In this experiment, SDS plays an important role in controlling the lateral growth of the nanorods. The surfactant molecules at a higher concentration are believed to form rod-like micelles (Guo *et al* 2002; Xiong *et al* 2002; Lv *et al* 2004; Zhang *et al* 2004) which might have formed by entrapping the Zn^{2+} and OH^- ions, already present in the reaction medium, forming rod shaped $Zn(OH)_2$. These rod like micelles are stable at low temperature (Guo *et al* 2002; Zhang *et al* 2004) ($< 100°C$) and during the period of refluxing, the $Zn(OH)_2$ molecules within the micelles begin to decompose. Also, the elevated temperature may have increased the activity of SDS and the micelles to collide with each other and thus increase the length of the nanorods. It can be seen from figures 3e and f, that there was an increase in length only, when the period of refluxing was increased from 3–5 h. However, in addition to the above-mentioned mechanism the possibilities of other mechanisms responsible for the restriction of the lateral growth cannot be ruled out. For example, it is also possible that instead of forming rod like micelles, the surfactant molecules get absorbed on the side surface of ZnO

nanorods (Sun *et al* 2002) restricting the lateral growth. The question that remains at this stage is, why should the diameter of the nanorods increase with increasing pH of the solution. The increase in pH of the solution leads to the formation of more $Zn(OH)_2$ and thus increase the concentration of $Zn(OH)_2$ in the solution. So, if there exists a concentration difference of $Zn(OH)_2$ between the inside and outside of the rod like micelles, there may be a transfer of $Zn(OH)_2$ from outside to inside the micelles through the surface of the micelles (Xiong *et al* 2002) and thus increase the diameter of the resulting nanorods. The experiments demonstrated in this paper clearly indicate that the columnar structure of ZnO could be formed in the solution without SDS (figure 3a) but the lateral dimension becomes too large as compared to the samples prepared with SDS. So the effect of SDS was to confine lateral growth so that high aspect ratio of the nanorods can be achieved. The synthesis approach described here is also suitable to vary the length of the nanorods within a wide range by using proper amount of hydrazine hydrate.

4.3 *Optical properties*

Figure 7a shows the room temperature optical absorbance spectra of *c*-axis oriented ZnO thin film and the aligned ZnO nanorods arrays. A sharp absorption edge at 368 nm corresponding to 3·37 eV was observed from both the samples. This corresponds to bulk values of the bandgap of ZnO. The absorption study also revealed that the as-prepared ZnO nanorod arrays are transparent in the visible region. Photoluminescence (PL) property of ZnO was widely investigated for its potential applications in UV photonic devices. This is also an important tool to evaluate crystal defects. The room temperature photoluminescence spectra of the as prepared ZnO thin film and the nanorod arrays are shown in figure 7b. The photoluminescence spectra of all the samples show very strong emission at 3·22 eV, which is generally attributed to the excitonic emission (Liang *et al* 2005). It was also observed that the intensity of the excitonic emission depends on the degree of alignment of the ZnO nanorods. It was observed that the intensity of the UV emission peak was maximum for sample S2 having best alignment and least for the randomly oriented nanorods in sample S5. The intensity of the emission from the ZnO thin films were quite low compared to the nanorod arrays and the PL plot of the ZnO thin film was multiplied by a factor for better visibility. It can be observed that in addition to the excitonic emission, the photoluminescence spectrum of ZnO film consists of a broad emission in the visible green region (figure 7b). This green light emission peak originated due to transition from defect states (Roy *et al* 2003; Kar *et al* 2006). However, this defect level emission was very weak in the photoluminescence spectrum of ZnO nanorods. So it is clear that the defect concentration could be

substantially reduced by this synthesis approach. The PL studies of the ZnO nanorod (Hsu *et al* 2004), nanowire (Lyu *et al* 2002) and nanonail (Kar *et al* 2006) arrays produced by high temperature based thermal evaporation approach revealed that these arrays exhibited a strong defect related emission band along with the excitonic UV emission. Thus ZnO nanorod arrays having good UV emission property could be synthesized by this surfactant assisted approach.

4.4 *Field emission properties*

For the field emission measurement, the ZnO nanorod arrays having the best alignment and well-separated
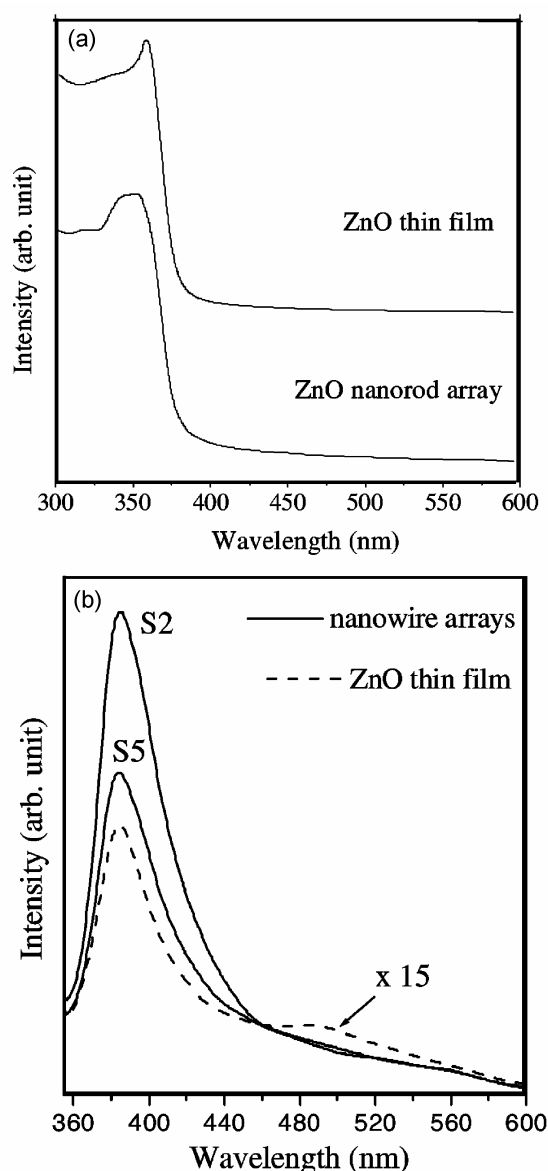

Figure 7. Room temperature optical absorption spectra of (**a**) the ZnO thin film with preferred crystallographic orientation and (**b**) photoluminescence spectra of the *c*-axis oriented ZnO films before and after the formation of ZnO nanorod arrays.

nature (S2) was arranged in two parallel plate configurations in a vacuum chamber with a pressure of 10^{-7} Torr and the distance between the electrodes was maintained at 300 μm. The measured current density as a function of electric field is shown in figure 8a. A very low turn-on electric field of 1·7 V/μm was obtained at an emission current density of 0·1 μA/cm², which reaches to 10 μA/cm² at an electric field of 1·9 V/μm. This value of turn-on electric field is significantly lower than ZnO nanopencils (Calleja and Cardona 1977), ZnO nanoneedles (Li *et al* 2004), and ZnO nanorods coated with amorphous carbon (Liao *et al* 2005). According to Fowler–Nordheim (F–N) model, the electron emission from a semi-infinite flat metallic surface can be expressed in terms of current density (*J*) and electric field, *E*, as

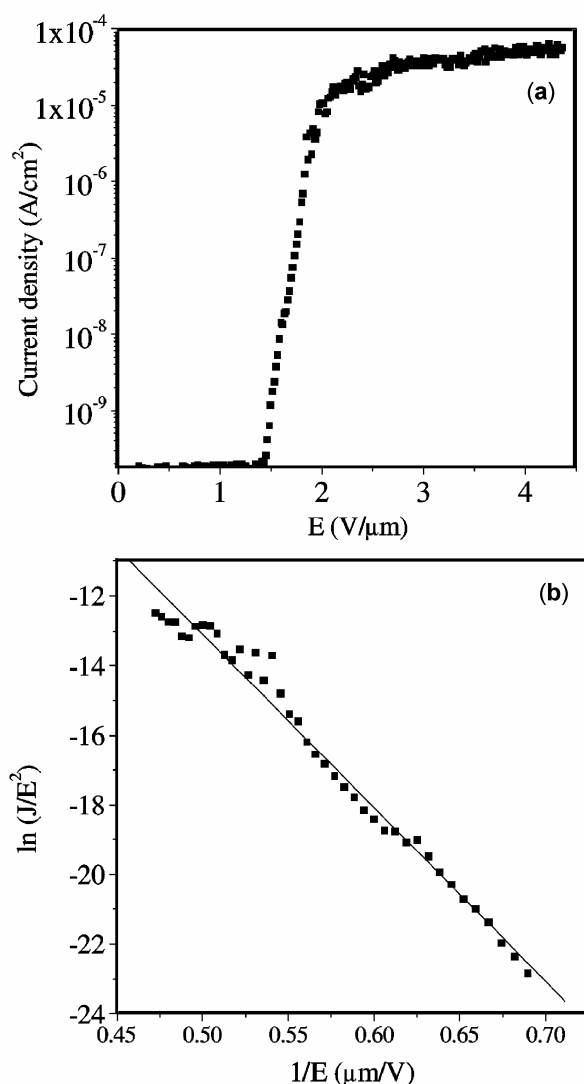$$J = A(\beta^2 E^2/\varphi)\exp(-B\varphi^{3/2}/\beta E), \qquad (1)$$

Figure 8. (**a**) *J–E* plot of the field emission from the ZnO nanorod array having best orientation and (**b**) corresponding *F–N* plot.

where *A* and *B* are constants, $A = 1·54 \times 10^{-10}$ (AV⁻² eV), $B = 6·83 \times 10^{9}$ (Vm⁻¹ eV⁻³ᐟ²) and *φ* the work function. *β*, the field enhancement factor of the sample, is associated with the magnitude of the electric field at the emitting surface by the relation

$$E(\text{local}) = \beta E,$$

where *E* (local) is the local electric field at the emitting top surface. Figure 8b shows the plot of $\ln(J/E^2)$ vs $1/E$, exhibiting linear dependencies, which is in agreement with (*F–N*) model (eq. (1)). The value of field enhancement factor, *β*, can be estimated from the slope of the (*F–N*) plot if the value of work function, *φ*, is known. If we assume the work function (*φ*) as 5·3 eV, the value of *β* is calculated to be ~1730, which is much higher than other recent reports on ZnO (Cui *et al* 2005; Ham *et al* 2005). The field enhancement factor usually depends on the geometry, tip size, length and number density of the nanorods grown on a substrate (Li S Y 2004). For high aerial density of nanorods the local field at the emitting surface reduces due to the electrostatic screening effect provoked by the neighbouring nanorods. On the other hand, long and highly oriented nanorods exhibit much better field emission than short and randomly oriented nanorods (Nilsson *et al* 2000; Banerjee *et al* 2004). The vertical growth of the ZnO nanorods have better ability to enhance local field at the emitting surface and reduce the turn on electric field (Banerjee *et al* 2004). The excellent field emission property of as-prepared ZnO nanorod arrays can be attributed to their good orientation and high aspect ratio.

5. Conclusions

We have successfully prepared ZnO thin films with a preferred *c*-axis texturing by sol–gel technique and fabricated well-aligned ZnO nanorod arrays with tunable length up to 6 μm on these ZnO films by using a simple surfactant-assisted approach. Diameters of the nanorods have been successfully reduced by using surfactant. Well-aligned ZnO nanorod arrays can be prepared over any substrate so long as a *c*-axis textured uniform ZnO film can be grown on it. High uniformity of the arrays can also be maintained over a large area by this novel approach. The optical properties of as-prepared nanorod arrays show their good crystalline quality. These films of long and aligned ZnO nanorods also exhibited very efficient field emission properties with a turn-on field as low as 1·7 V/μm and a high field enhancement factor (*β*). These films of highly oriented nanorod arrays have potential applications in photonics, field emission displays, nanoelectronics and gas sensing devices.

References

Bae S Y, Seo H W and Park J 2004 *J. Phys. Chem.* **B108** 5206

Banerjee D, Ho S J and Ren Z F 2004 *Adv. Mater.* **16** 2028

Baughman R H, Zakhidov A V and de Heer W A 2002 *Science* **297** 787

Calleja J M and Cardona M 1977 *Phys. Rev.* **B16** 3753

Cui J B, Daghlian C P, Gibson U J, Püsche R, Geithner P and Ley L 2005 *J. Appl. Phys.* **97** 044315

Dev A, Kar S, Chakrabarty S and Chaudhuri S 2006 *Nanotechnology* **17** 1533

Fancher C A, de Clercq H L, Thomas O C, Robinson D W and Bowen K H 1998 *J. Chem. Phys.* **109** 8426

Gao P X and Wang Z L 2004 *J. Phys. Chem.* **B108** 7534

Greene L E, Law M, Goldberger J, Kim F, Johnson J C, Zhang Y, Saykally R J and Yang P 2003 *Angew. Chem. Int. Ed.* **42** 3031

Greene L E, Law M, Tan D H, Montano M, Goldberger J, Somorjai G and Yang P 2005 *Nano Lett.* **5** 1231

Guo L, Ji Y L, Xu H, Simon P and Wu Z 2002 *J. Am. Chem. Soc.* **124** 14864

Ham H, Shen G, Cho J H, Lee T J, Seo S H and Lee C J 2005 *Chem. Phys. Lett.* **404** 69

Hsu N E, Hung W K and Chen Y F 2004 *J. Appl. Phys.* **96** 4671

Huang M H *et al* 2001 *Science* **292** 1897

Kar S, Pal B N, Chaudhuri S and Chakravorty D 2006 *J. Phys. Chem.* **B110** 4605

Liang J, Liu J, Xie Q, Bai S, Yu W and Qian Y 2005 *J. Phys. Chem.* **B109** 9463

Liao L, Li J C, Wang D F, Liu C S, Fu Q and Fan L X 2005 *Nanotechnology* **16** 985

Li Q, Kumar V, Li Y, Zhang H, Marks T J and Chang R P H 2005 *Chem. Mater.* **17** 1001

Li S Y, Lin P, Lee C Y and Tseng T Y 2004 *J. Appl. Phys.* **95** 3711

Li Y B, Bando Y and Golberg D 2004 *Appl. Phys. Lett.* **84** 3603

Li Z, Ding Y, Xiong Y, Yang Q and Xie Y 2004 *Chem. Eur. J.* **10** 5823

Lv R, Cao C, Guo Y and Zhu H 2004 *J. Mater. Sci.* **39** 1575

Lyu S C, Zhang Y, Ruh H, Lee H J, Shim H W, Suh E K and Lee C J 2002 *Chem. Phys. Lett.* **363** 134

Lyu S C, Zhang Y, Lee C J, Ruh H and Lee H J 2003 *Chem. Mater.* **15** 3294

Milne W L *et al* 2004 *J. Mater. Chem.* **14** 933

Nilsson L *et al* 2000 *Appl. Phys. Lett.* **76** 2071

Pan Z W, Mahurin S M, Dai S and Lowndes D H 2005 *Nano Lett.* **5** 723

Park W I, Kim D H, Jung S W and Yi G C 2002 *Appl. Phys. Lett.* **80** 4232

Roy V A L, Djurisic A B, Chan V, Gao J, Lui H F and Surya C 2003 *Appl. Phys. Lett.* **83** 141

Saito Y and Uemura S 2000 *Carbon* **38** 169

Senda S, Sakai Y, Mizuta Y, Kita S and Okuyama F 2004 *Appl. Phys. Lett.* **85** 5679

Sun X M, Chen X, Deng Z and Li Y D 2002 *Mater. Chem. Phys.* **78** 99

Wang X D, Summers C J and Wang Z L 2004 *Nano Lett.* **4** 423

Wang Z L 2004 *Mater. Today* **7** 26

Xiong Y, Xie Y, Yang J, Zhang R, Wu C and Du G 2002 *J. Mater. Chem.* **12** 3712

Yu H, Zhang Z, Han M, Hao X and Zhu F 2005 *J. Am. Chem. Soc.* **127** 2378

Zhang J, Zhang S Y and Chen H Y 2004 *Chem. Lett.* **33** 1054